Postprint of: Miszczyk A., Darowicki K., Stratification of nano-pigments in anti-corrosive coatings by means of magnetic field, Progress in Organic Coatings, Vol. 147 (2020), 105869,
DOI: 10.1016/j.porgcoat.2020.105869

Stratification of nano-pigments in anti-corrosive coatings by means of magnetic field

A. Miszczyk*, K. Darowicki

Gdansk University of Technology, Chemical Faculty

Department of Electrochemistry, Corrosion and Materials Engineering

11/12 Narutowicza St., 80-233 Gdansk, Poland

*Corresponding author.

E-mail address: andrzej.miszczyk@pg.edu.pl

Abstract

The concept of self-stratification of coatings, although attractive, causes difficulties in its practical use, especially when pigments are added to the resins. An alternative way of obtaining a multilayer structure in a single step was presented. Using the inhomogeneous magnetic field and magnetically active components of the coating, the possibility of vertically graded differentiation of the one layer properties has been verified. For this purpose, the magnetic properties of nickel ferrite ($NiFe_2O_4$) nano-particles and magnetic field for their transport in a wet coating were used.

It has been shown that it is possible to use the magnetic field to transport magnetic ferrite, used as active anti-corrosive pigments, near the coating/substrate interface, in the initially homogeneous wet paint layer, during film formation. These results prove that magnetic ferrite pigments can be magnetically manipulated in liquid coating layer applied on the substrate. Using the impedance spectroscopy technique, it was possible to detect stratification by analyzing complex capacity diagrams. As a result of impedance tests, better anti-corrosive properties of the system hardened in the presence of the magnetic field were demonstrated.

Keywords: protective coatings; stratification; magnetic pigments; ferrites; EIS

1. Introduction

Organic coatings are an effective protection method against corrosion. Usually, to obtain good protection, a multi-layer coating system is required [e.g. 1-3]. This is due to the need to balance multiple (sometimes conflicting) requirements [4]. Therefore, the application of the coating system involves a multi-step application process resulting in vertically structured films with the layers having different composition and properties. On the other hand, these activities are time consuming, costly and create opportunities for adverse events deteriorating protective abilities of the system. In this way, an attractive concept was developed combining the advantages of a multilayer system and a single application of a coating by self-stratification phenomenon [5-9]. The condition for self-stratification is the mixing at least two immiscible binders soluble in a common solvent or mixture of solvents. After application, during the evaporation of the solvent, the two binders separate themselves. However, this attractive concept encounters difficulties in practical implementation and requires further research.

This article proposes a new approach to achieving pigment stratification inside the coating through the use of magnetic fields and pigments exhibiting magnetic properties. It consists of the controlled placement of these pigments in a specific place of the once applied coating layer. Targeted delivery of active anti-corrosive particles in the wet coating layer near the protected substrate using magnetic fields may be an area of interest in a specific situation. Anti-corrosive properties of magnetic ferrite micro- and nano-particles allow them to be used directly for this purpose. This does not exclude the use of other magnetic particles that do not possess active anti-corrosive properties. Then, they can be treated as carriers of other particles exhibiting features of active anti-corrosive pigment but not exhibiting magnetic activity.

Ferrites have the general formula MFe_2O_4, where M is a metal in a bivalent state, e.g., Fe^{2+}, Zn^{2+}, Ni^{2+}, Co^{2+}, Mn^{2+}, Cu^{2+} [10-13]. Depending on the type of metal, magnetic (e.g. Fe^{2+}, Ni^{2+}, Co^{2+}, Mn^{2+}) or non-magnetic (e.g. Zn^{2+}, Ca^{2+}, Cu^{2+}) ferrites may be obtained. Magnetic targeting allows ferrite particles to be concentrated and held at target sites like coating/steel interface in the coating body. This creates a characteristic structure for a layered or graded protective coating system. Externally controlled, site-specific particles

delivery would improve protective efficiency of the coating system by increasing the pigment concentration at the substrate, as well as decreasing the total amount of pigment required, reducing costs and the potential hazard to the environment. These benefits make magnetic targeting especially attractive for special areas that are difficult to properly protect with coatings such as edges, crevices, welds and joints.

. In this work, the effect of external inhomogeneous magnetic field on nano-ferrite particle movement in the coating layer was investigated to target magnetic pigment particles to the desired location that is around the coating/substrate interface.

2. Background

An external inhomogeneous magnetic field can induce movement of particles in a liquid matrix solution. The magnitude of the magnetic force depends on the magnetic nature of the particle material. In the case of para- and ferromagnetics, the presence of unpaired electrons in atomic orbits is characteristic [14-16]. Electrons have spin, which is associated with the existence of magnetic moment. Paired electrons reduce mutually existing moments, while unpaired electrons do not reduce. Under typical conditions and the absence of an external magnetic field, these moments are oriented randomly without giving a macroscopic magnetic effect. In the external magnetic field, these dipoles orient themselves along the magnetic field lines and macroscopic magnetization is observed.

Magnetization M is proportional to the properties of the particle material, represented by χ and the strength of the external magnetic field H, according to formula (1) [13-15]:

$$\mathrm{M} = \chi \mathrm{H}, \qquad (1)$$

where:

χ – the dimensionless magnetic susceptibility of the material,

H – the magnetic field strength (A/m^{-1}).

Due to the existence of thermal movements, this order is not complete. Under the inhomogeneous magnetic field, magnetized particles will migrate in the direction of increasing magnetic field. This occurs when the particle material is para- or ferromagnetic.

When the coating layer dries in a non-homogeneous magnetic field and it is in liquid form, the following forces act on the magnetic ferrite particle in the binder matrix: magnetic force F_m, gravity force F_g, viscous force F_v, buoyancy force F_b, particle interaction force F_i, and Brownian force F_B. This leads to the following general vector equation, resulting from Newton's second law [17]:

$$m\frac{d\vec{v}}{dt} = \overrightarrow{F_m} + \overrightarrow{F_g} + \overrightarrow{F_v} + \overrightarrow{F_b} + \overrightarrow{F_i} + \overrightarrow{F_B} \qquad (2)$$

where: m - particle mass,

v - particle speed,

dv/dt - particle acceleration.

To simplify this equation, it can be assumed that the gravitational force and the buoyancy force are balanced. Due to the particle size and their typical content (volume fraction) in the coating, Brownian force and the force of interaction between ferrite particles can be neglected. Then equation (2) is simplified to the following form:

$$m\frac{d\vec{v}}{dt} = \overrightarrow{F_m} + \overrightarrow{F_v} \qquad (3)$$

This means that only two forces act essentially on the particle: magnetic force and viscous force, as shown in Fig. 1.

The particle is exposed to the force of viscosity F_v when it moves in a liquid, according to the Stokes formula [18]:

$$F_v = 6\pi R\eta\frac{dx}{dt}, \qquad (4)$$

where:

R – the radius of the particle,

η – the dynamic viscosity,

dx/dt – the speed of particle movement, the position change with respect to time.

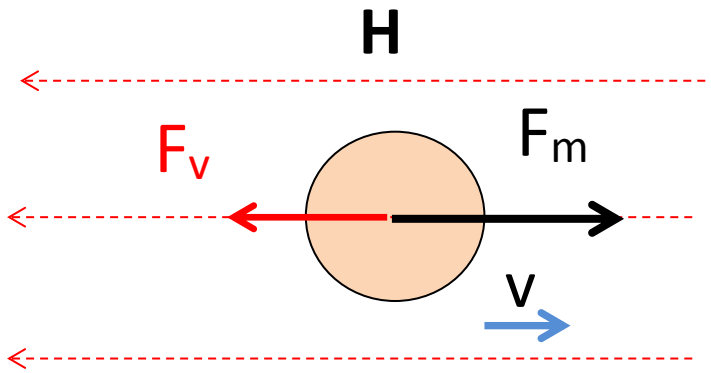

Fig. 1. An image of forces acting on a ferrite particle in a wet coating layer in an inhomogeneous magnetic field.

The formula shows that it is proportional to the speed of particle movement. When the magnetic force ceases, viscous force disappears and the particle is located where it was at this moment.

The magnetic force can be written as [14-17]:

$$\overrightarrow{F_m} = \frac{\chi}{\mu_0} V(\vec{B} \cdot \vec{\nabla})\vec{B}, \qquad (5)$$

where:

μ_0 – the magnetic permeability of vacuum ($4\pi\ 10^{-7}$ Hm^{-1}),

V – the volume of the particle,

B – the magnetic field,

$\vec{\nabla}B$ – the magnetic field gradient.

This equation shows that a magnetic field gradient is required to exert a translation force on a particle. In a homogeneous field, the particle will be forced to take its place only along the direction of the magnetic field.

Fig. 2 presents the idea of delivery of magnetic pigment particles inside the wet coating to the interface between the coating and the substrate in a magnetic field.

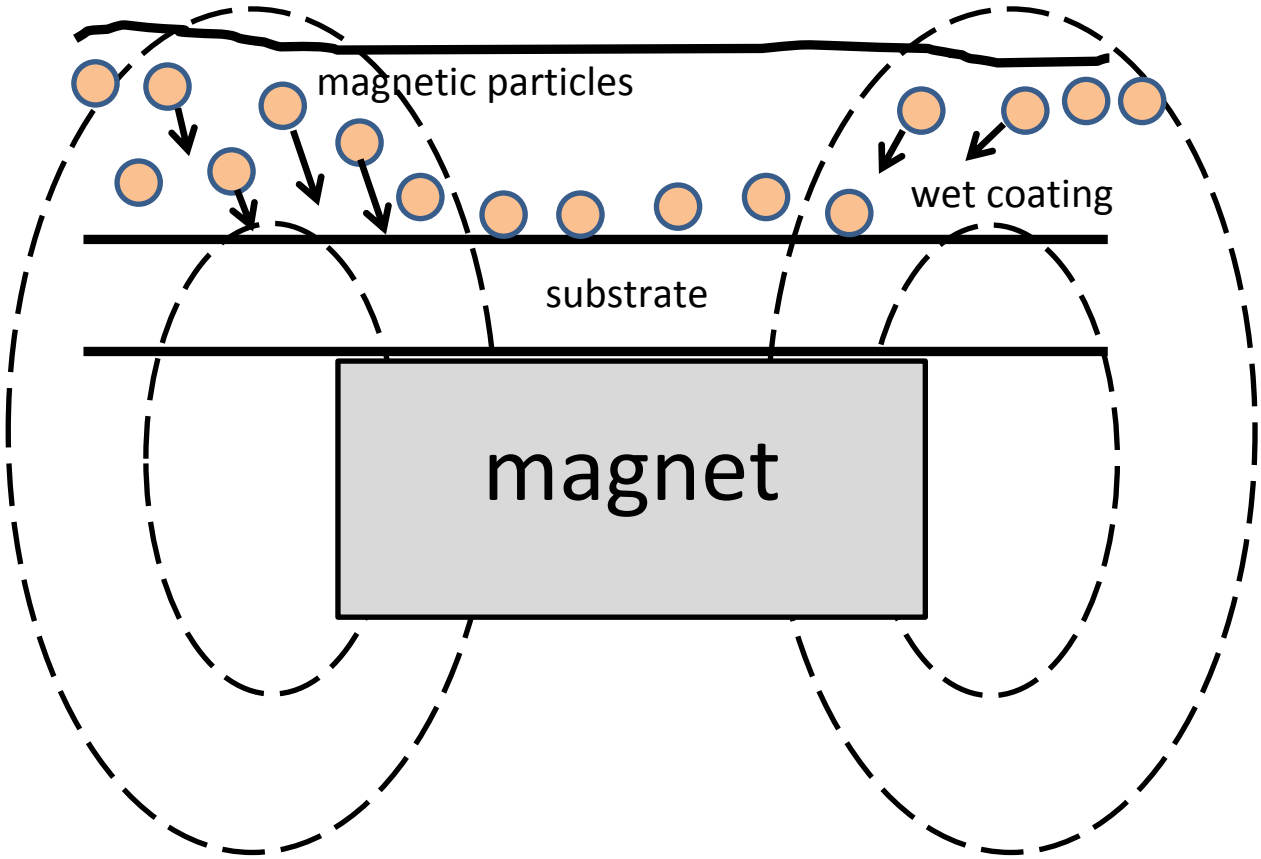

Fig. 2. Schematic behaviour of magnetic pigment particles inside the wet coating layer in the inhomogeneous magnetic field.

3. Experimental

To verify the concept of magnetic pigment stratification within the coating layer in the magnetic field, nickel ferrite was used. Nickel ferrite $NiFe_2O_4$ was synthesized by using the co-precipitation method [19]. The starting materials were reagent grade purity nitrates $Fe(NO_3)_3 \cdot 9H_2O$ and $Co(NO_3)_3 \cdot 6H_2O$. Desired amounts of $Fe(NO_3)_3 \cdot 9H_2O$, $Zn(NO_3)_3 \cdot 6H_2O$ and $Ni(NO_3)_3 \cdot 6H_2O$ were mixed to yield a clear aqueous solution. The mixed solution was placed in a water bath at 90 ^oC, and then NaOH solution (6 mol/l) was added dropwise with intensive stirring. The precipitation occurred immediately to change the reaction solution to dark grey. During the precipitation, the reaction solution was vigorously stirred with a magnetic stirrer. After reaction completion, the precipitates were kept stirred in the reaction solution for 2 h at a temperature of 90 ^oC. The co-precipitated powders were filtered and

washed with deionized water many times, followed by washing with ethyl alcohol and filtering. The washed powders were dried at 80 °C during 24 h. The precipitate was calcined at 600 °C for 2 h and ground in a ball mill for 2 h. The obtained ferrite nanoparticles show magnetic properties, Fig. 3. For comparison, nickel ferrite was also obtained by the traditional ceramic method, described in detail in [12]. Briefly, the weighed amounts of the above-mentioned salts were dry mixed in a laboratory ball mill for two hours. Then, the obtained mixture was transferred to a crucible and baked at 1200 °C for 2 hours. After the furnace had cooled, the crucible content was crushed in a ball mill for 5 hours. The ferrite dust obtained is further rinsed with water and dried.

White Evonik Aeroxide TiO2 P25 pigment was added to some of the samples to visualize the effects of stratification.

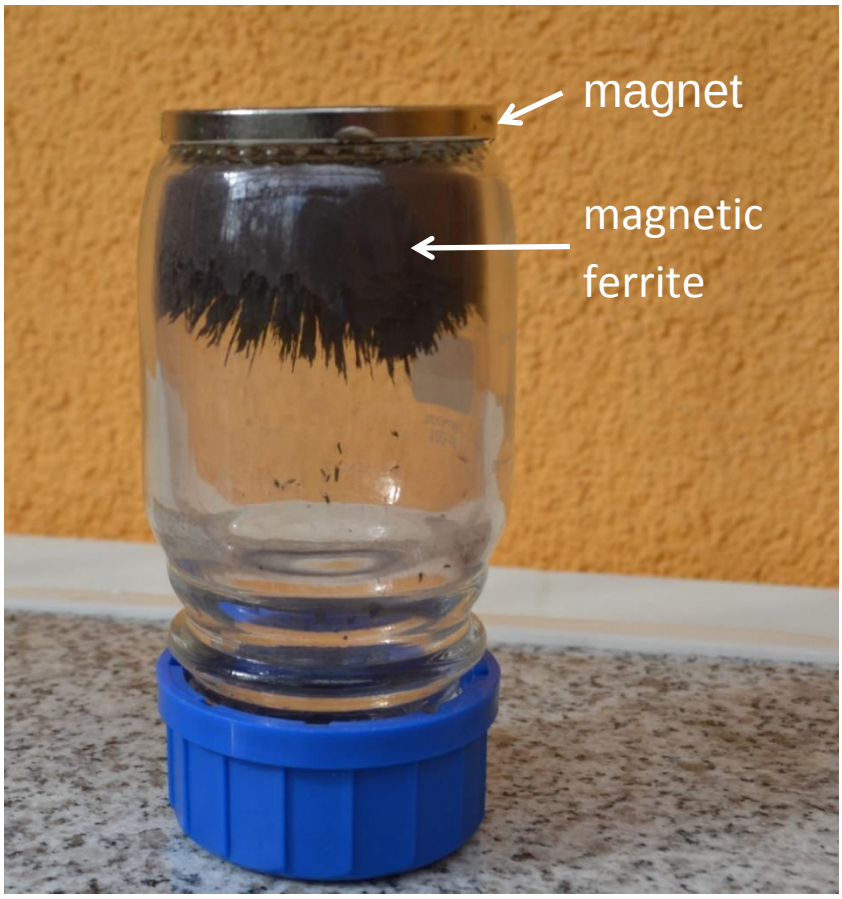

Fig. 3. The magnetization of the nickel ferrite nano-particles in the magnetic field of the permanent magnet.

Coating material has been prepared by mixing ferrite particles with an epoxy resin (Epidian-5, from Sarzyna-Organika Chemical Company in Nowa Sarzyna, Poland, clear epoxy resin with molecular mass ≤ 700u, glycidyl ether of bisphenol A) using stirrer during 1 h (800 turns per minute). The epoxy resin with ferrite powder was then sonicated for 15 minutes at a temperature of about 40 °C to disperse the pigment more precisely and remove air bubbles. Next, the hardener (Z1 from Sarzyna-Organika Chemical Company in Nowa Sarzyna, Poland, triethylenetetramine) was added in a weight ratio of 1: 0.12 following the manufacturer's instructions. After mixing, a coating was applied to the steel substrates side by side with the applicator. The steel surface before painting was cleaned with sandpaper up to number 400, washed with demineralized water, dried and degreased with acetone. Composites containing 5 vol.% of ferrites were prepared on a low carbon steel (S235JR) substrate (1mm thick). The thickness of all coatings was about 500 μm.

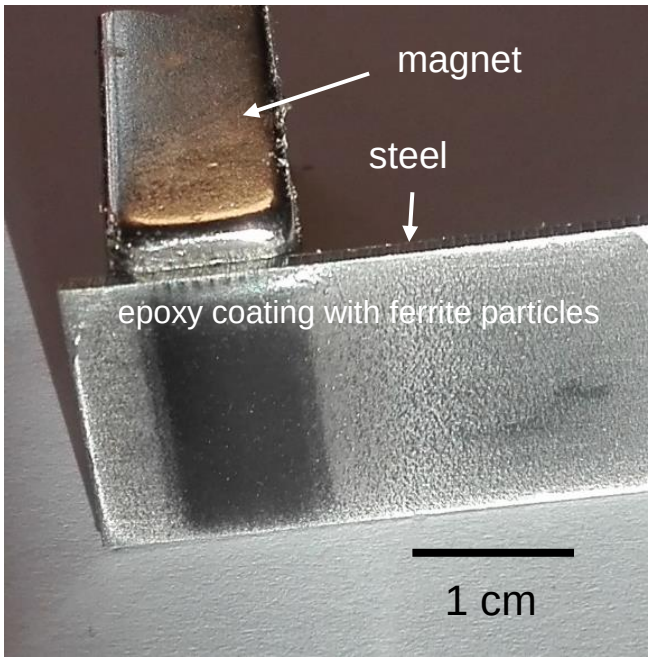

Fig. 4. Effect of the magnetic field on ferrite particles contained in an epoxy coating.

To create the magnetic field, neodymium permanent magnets with dimensions of 6 cm x 2 cm x 1 cm or in a round form with a diameter of 40 mm of the N52 type were used to obtain a magnetic field of 0.15 T near the tested samples measured by magnetic sensor SMS 102 (Asonik, Poland), Fig. 4. To obtain samples with larger surfaces, a steel substrate was shifted with an unhardened coating, using the system shown in Fig. 5. A short-term interaction is

sufficient to properly positioning the pigment. Curing of the coatings took place in laboratory conditions (22 (±2) °C, 45-50 % RH).

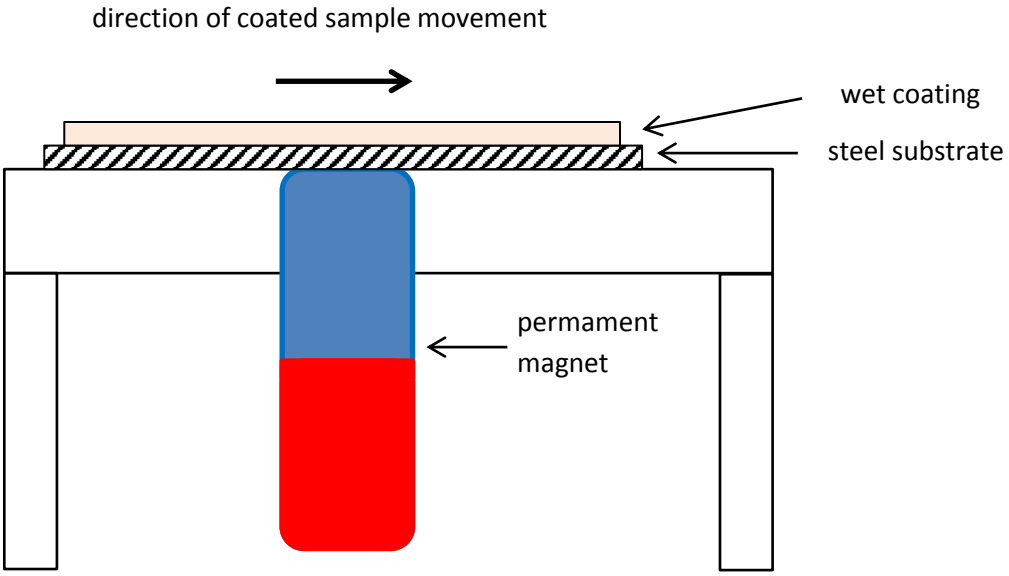

Fig. 5. Schematic system for magnetic field interaction on a wet (not hardened) coating layer.

The two-electrode electrochemical cell consisted of the coated carbon steel (S235JR) sample with an exposed area of 4.5 cm^2 was used as a working electrode and a platinum mesh as a counter electrode. Electrochemical measurements were made using ModuLab XM ECS (Solartron Analytical - Ametek SI). Impedance spectra were obtained in the frequency range of 1 MHz to 0.01 Hz with 10 points per decade in the frequency range 1 MHz–1 Hz and 5 points per decade below 1 Hz, using 60 mV (intact coatings) or 20 mV (coatings with artificial defect) perturbation signal amplitude. The coated panels were exposed in the laboratory to immersion in dilute Harrison's solution (aqueous solution of 0.35% $(NH_4)_2SO_4$ and 0.05% NaCl) at 22(±1) ^oC. Dilute Harrison`s solution was chosen as a corrosive environment because it has become a standard environment modelling atmospheric corrosion. It was originally developed following investigations of atmospheric pollution and contamination found in an atmosphere close to railway train tracks. As a result of these investigations, Harrison used as a solution a mixture of the ammonium sulphate (3.25 wt%.) and sodium chloride (0.25 wt%) [20]. Later, based on the tests, Timmis proposed a 10-times diluted solution [21, 22]. Its usefulness was confirmed by its use as the test solution for the Prohesion test cycle

following ASTM G-85. This test was introduced to the study of coatings, especially primer layers and active anti-corrosion pigments [21], to provide more realistic results compared to the salt spray chamber. Currently, this solution is often used to test various coatings on galvanized steel [23], aluminium and magnesium alloys [24-27].

Artificial damages in the coatings were introduced employing cutter, with the "V"-shaped cut in the form of a 1 cm single line segment in the centre of the exposed area. Impedance tests of the coatings took place about 3 weeks after application.

XRD analysis was performed on a Philips X'Pert diffractometer with Cu Kα radiation in the 2Θ range from 10^o to 90^o by steps of 0.02^o.

SEM images and EDX analysis of the sample cross-section were obtained using a scanning electron microscope (S-3400N, Hitachi) equipped with an X-ray dispersion spectrometer (EDX).

AFM studies were conducted using a commercial AFM device Ntegra Prima (NT-MDT, Russian Federation) supplemented with a magnetic tip. In this case, the magnetic forces, acting on a magnetized tip by the sample, are measured and local magnetic properties of the surface in the form of a map were registered.

4. Results and Discussion

Characterization of the obtained ferrite nano-particles was carried out by X-ray diffraction (XRD) analysis. Fig. 6 shows a comparison of the XRD pattern of the traditional ceramic ferrite (calcined at 1200 ^{o}C) with the same one obtained by co-precipitation method and calcined at 600 ^{o}C. There are no essential differences between them regarding the location of the peaks [13, 28]. Differences in peak width are associated with different particle sizes (macro- particles versus nano-particles) [29].

Epoxy coatings, containing 5 vol% addition of magnetic ferrite nano-particles without and in the presence of magnetic field curing, were obtained. The permanent magnet generates a heterogeneous magnetic field with a gradient directed towards the substrate, which causes ferrite particles migration to the substrate. The obtained coating microstructure was observed on its cross-sections with a magnetic force microscope (MPM).

This is a variation of the AFM technique, in which the tip coated with a magnetic substance is used.

To separate other forces acting on the tip from the magnetic forces, a two-pass technique at different distances from the sample is used during imaging. For the first scan, contact mode is used to get the topography of the sample, similar to the process used in AFM. During the second scan, the cantilever tip is set at a small constant distance from the sample surface based on the first scan. At this altitude atomic forces are negligible and the tip only interacts with the magnetic force, which allows for imaging. During the second scanning, oscillations of the cantilever are changing phase due to the interaction with magnetic forces from the sample. Changing of the tip's oscillation phase creates an image of the surface in terms of magnetic properties.

Fig. 7 shows micrographs of cross-section scanning maps of topography (a) and magnetic properties (b) near the steel substrate. In both cases, the presence of nano-sized pigment particles can be seen. On the vertical axis of the second micrograph the change of the tip oscillation phase is shown (the unit is the degree (^{o})).

The used epoxy binder was almost transparent, so the stratification effect is not macroscopically clearly visible. To visualize the stratification caused by the magnetic field, about 3 vol% of titanium dioxide was added to the resin containing ferrite. All form (rutile, anatase, brookite) of TiO_2 are diamagnetic [30]. Therefore, its particles will not be susceptible to magnetic fields. As a result, the sample exposed to the magnetic field will become more white (titanium dioxide colour) due to the change in the position of dark grey ferrite (as a result of stratification). And this effect was observed, Fig. 8. The distribution of ferrite particles and titanium dioxide in the coating was also examined on the cross-section using the SEM-EDX technique. Fig. 9 presents distribution maps of iron (responsible for ferrite) and titanium (responsible for titanium dioxide) on the cross-section of the sample exposed to the magnetic field. In the case of titanium, we observe an even distribution in the volume of the coating, while in the case of iron, there is a concentration gradient. There is much more iron near the steel substrate than at further distances from the substrate.

To observe changes in the coating caused by the magnetic field impact, impedance tests were performed. Fig. 10 shows the diagrams of the impedance module and phase

(Bode format) for both coatings, obtained after 1 hour of exposure in dilute Harrison's solution. Measurement at the beginning of the exposure characterizes the coating by minimizing the effects of water absorption and swelling. Thanks to this, it allows characterizing the influence of the magnetic field in a reliable way. As can be seen from the course of the module spectra and the phase, both samples differ in capacities. Intrinsically, Bode impedance plots expose resistance relationships in the system under study. Therefore, it was decided to transform the obtained impedance data into the complex capacitance C to observe subtler differences, using the following formulas [31]:

$$C = C' + j\,C'' = 1/j\omega Z\,, \qquad (6)$$

$$C' = -\frac{Z''}{\omega(Z'^2 + Z''^2)}\,, \qquad (7)$$

$$C'' = -\frac{Z'}{\omega(Z'^2 + Z''^2)}\,, \qquad (8)$$

where: Z' and Z'' – real and imaginary part of impedance Z,

ω - the angular frequency.

The data in this form is shown in Fig. 11. It is seen that both graphs differ in capacities and in the case of a sample shaped in the magnetic field we observe a more complicated structure. For this sample, a widespread of the real capacity value is observed in the higher frequency range. For more accurate representation, the relationship between the real capacity and frequency (equivalent to Bode plots for impedance) is shown in Fig. 12. Here it is seen that the sample formed without magnetic field shows the presence of one capacity, while the one that arose in the magnetic field shows two capacities (cut-offs at the lowest frequencies on the vertical axis). In other words, a significantly greater dispersion of the electrical capacity of the coating is observed in the case of curing in a magnetic field than without the presence of a magnetic field, although the composition of both coatings is identical. It seems that such courses can be an indicator of the degree of stratification in general and, in this case as a result of the magnetic field application.

The influence of stratification of ferrite nano-particles in the coating under the influence of magnetic field on the protective properties of epoxy coatings was tested. Two nominally identical coatings were compared, one of which was subjected to a non-uniform

magnetic field during curing and the other without the presence of this field. To check the active effect of pigments in both situations, coating damage was made in the form of a scribe to the steel substrate and then the samples were immersed in dilute Harrison's solution. Impedance tests were performed 2 hours after immersion (Fig. 13) and after 4 weeks of immersion (Fig. 14).

The spectra in Fig. 13 show the state of both coatings at the beginning of the exposure. Both spectra are similar, which indicates that the incisions are very similar and the way they are made will not affect the final results. After 4 weeks of exposure (Fig. 14), a significant difference is observed. In general, the impedance values are much higher for a sample cured in a magnetic field. Comparing them with the spectra of Fig. 9, an increase in impedance is observed in both cases, which indicates the active, protective effect of the pigment.

The protective effect of ferrite pigments is mainly associated with the blocking of cathodic areas [11, 12]. In the presence of water, slight leaching of ions occurs on the surface of the ferrite particles, which in the alkaline environment of the cathode region causes the deposition of hydroxide layers of the corresponding metals released from the ferrite particles. This probably causes some increase in resistance in the pores (defects) of the coating by sealing the gaps around the defect between the coating and the substrate (effect of delamination). We can observe this on the impedance spectra as the increase in the diameter of the semi-circles responsible for the barrier properties of the coating (high-frequency range).

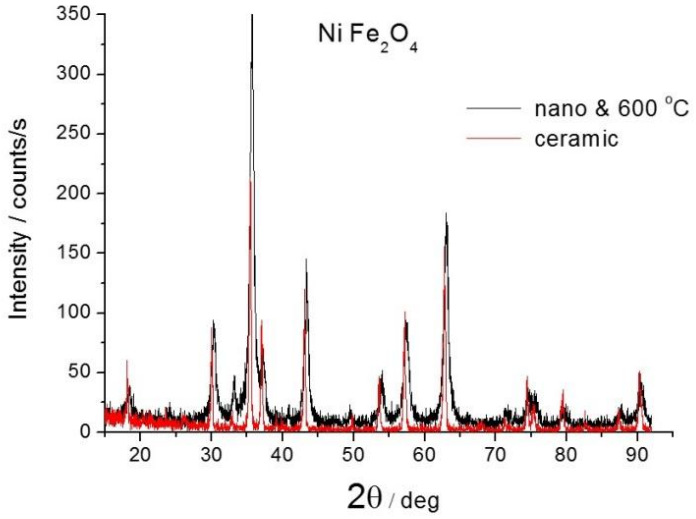

Fig. 6. Comparison of XRD pattern of $NiFe_2O_4$ ferrites obtained by ceramic method at 1200 °C or co-precipitation method and after annealing at 600 °C.

(a)

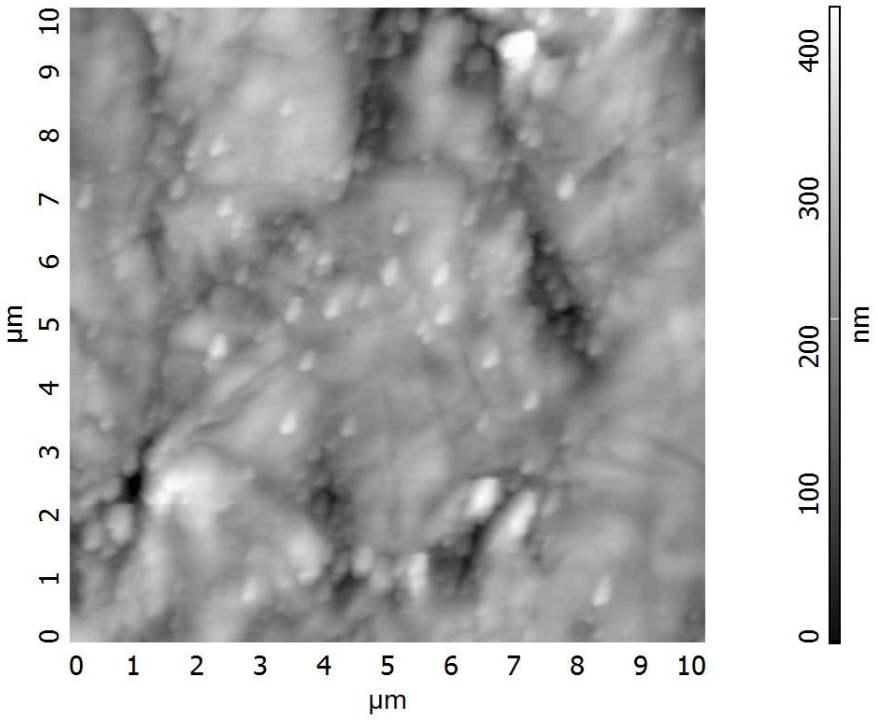

(b)

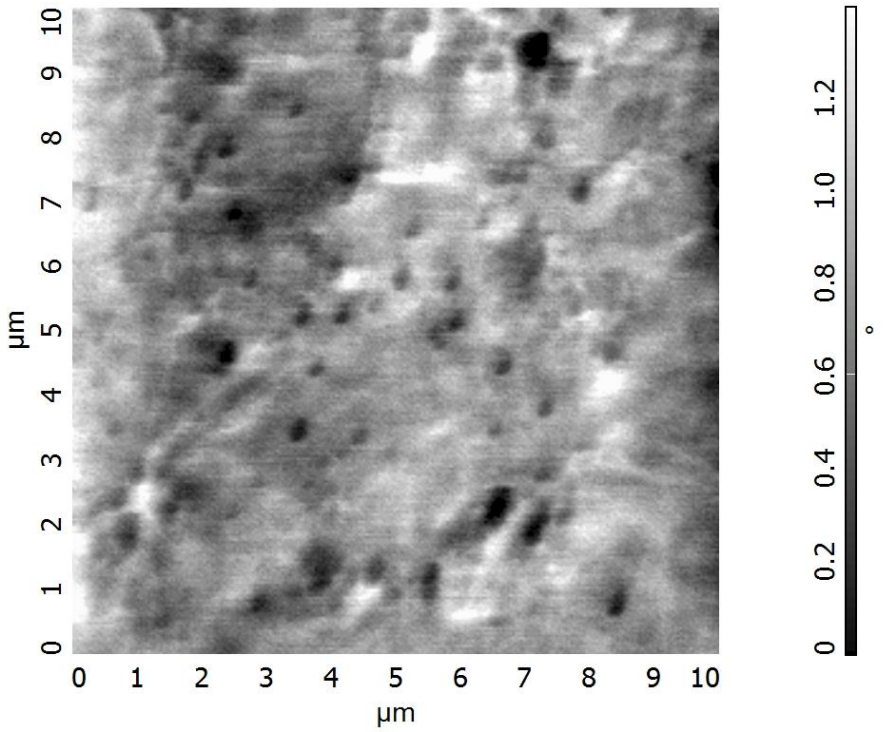

Fig. 7. AFM images of topography (a) and magnetic properties (b) on the cross-section of the coating near the steel substrate.

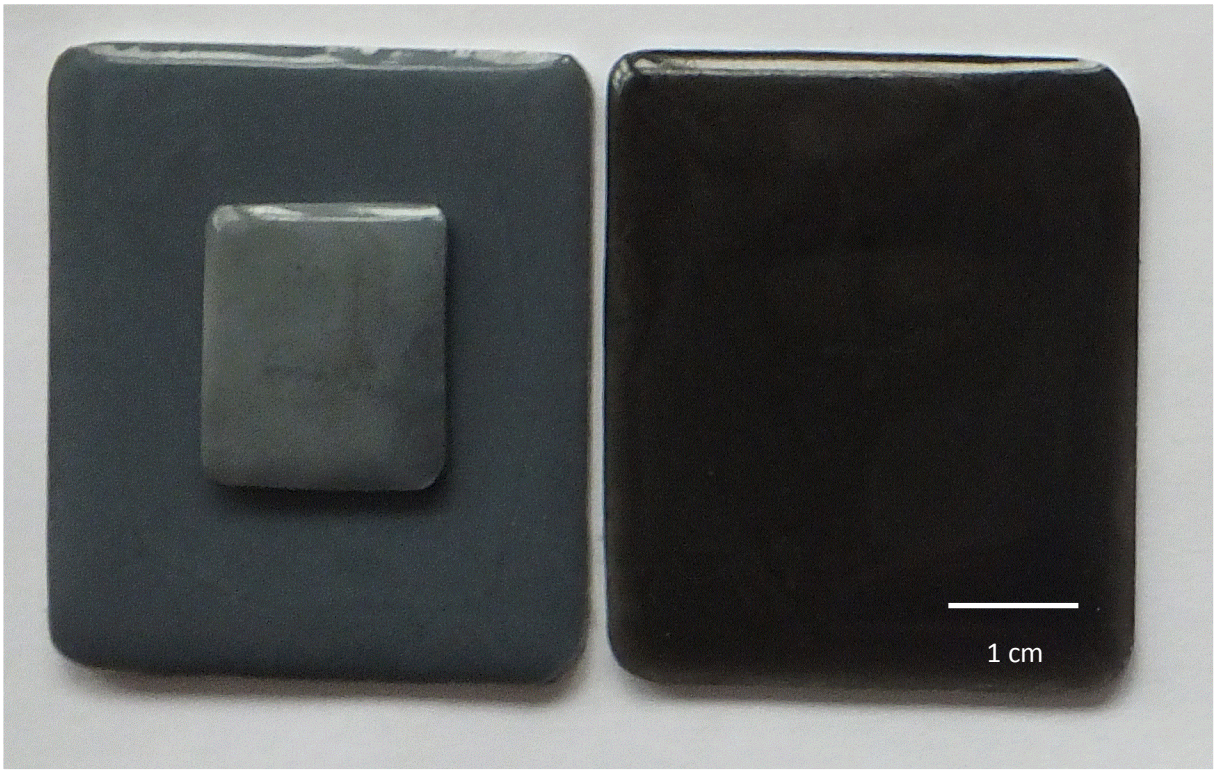

Fig. 8. Samples of epoxy coating on steel with ferrite only (right), with ferrite and TiO2 (left), the small sample was placed in a magnetic field, its brighter colour as a result of stratification caused by the magnetic field is observed.

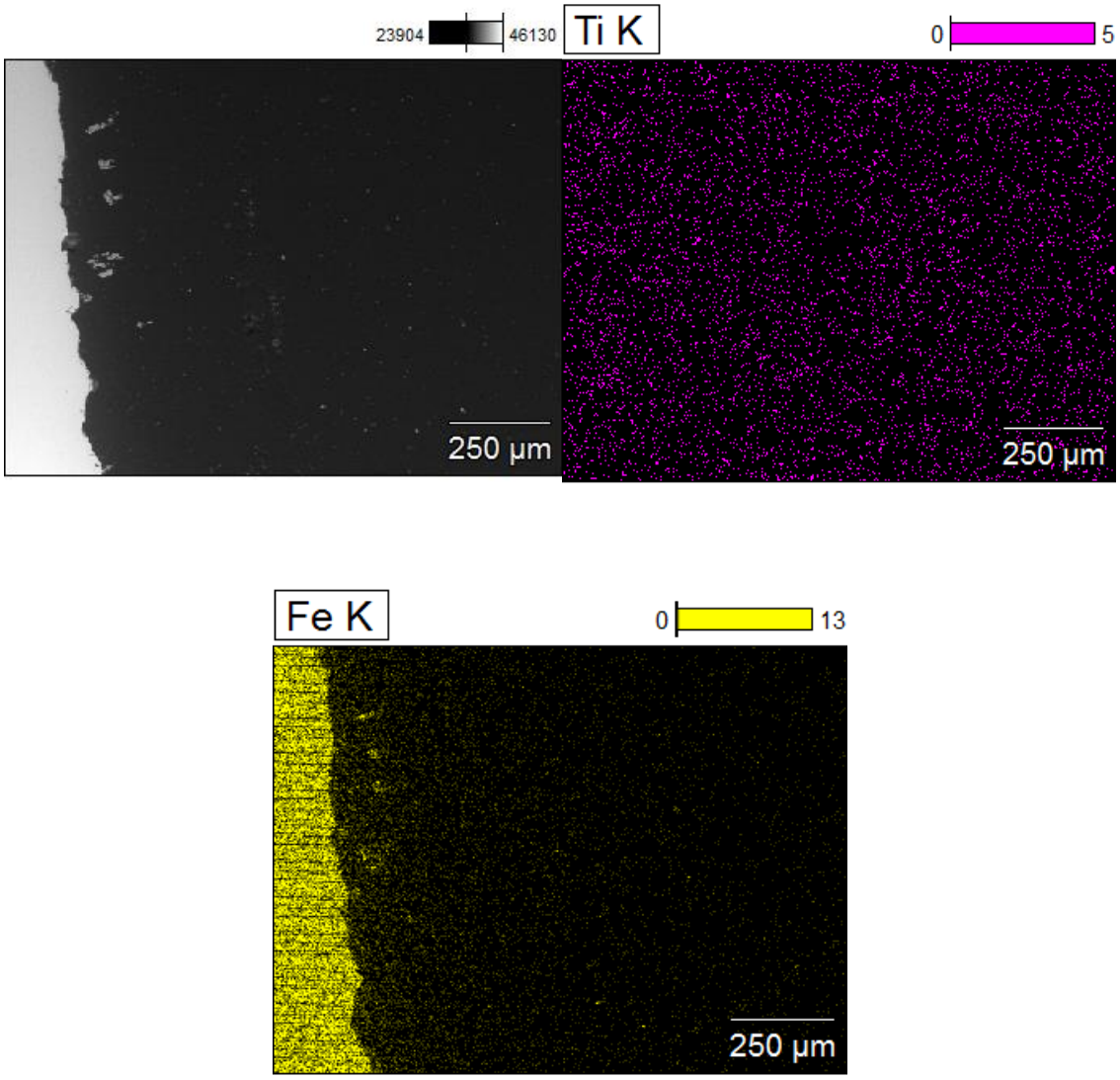

Fig. 9. SEM-EDX images of sample cross-section showing the Ti (purple) and Fe (yellow) contents after stratification in the magnetic field.

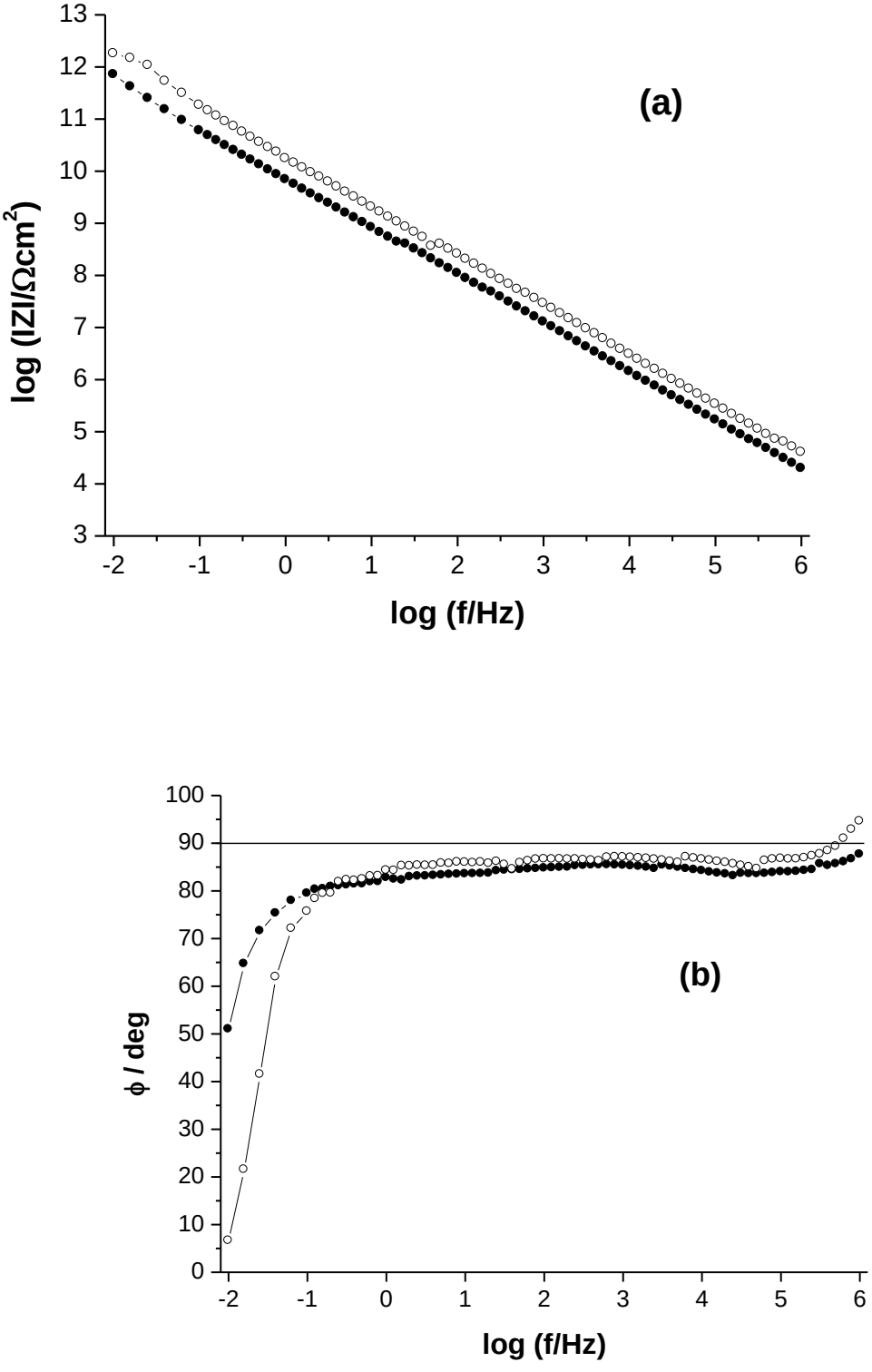

Fig. 10. Impedance spectra of modulus (a) and phase angle (b) in Bode format for the tested coating cured in the magnetic field (●) and without the magnetic field (o).

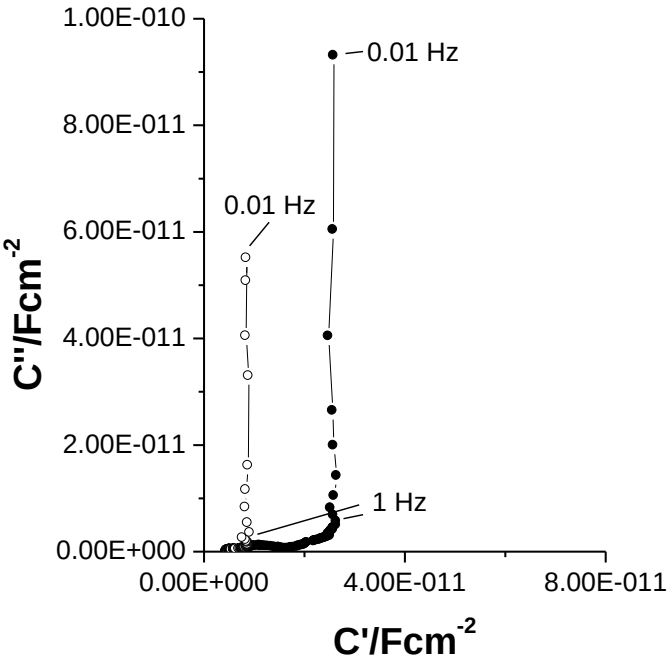

Fig. 11. Capacitance spectra for the tested coating cured in a magnetic field (●) and without a magnetic field (o).

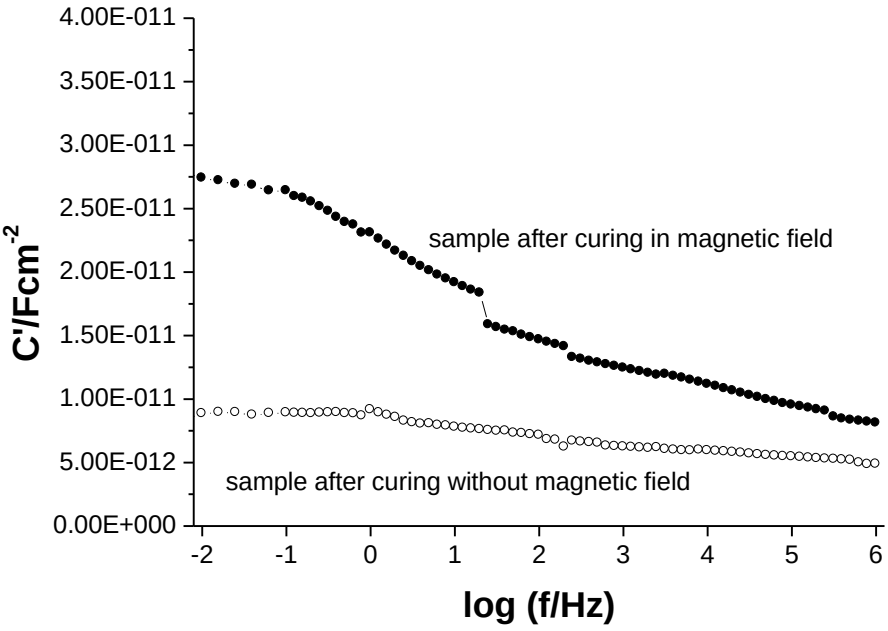

Fig. 12. Real capacitance spectra for the tested coatings cured (hardened) in a magnetic field (●) and without a magnetic field (o) as a function of frequency.

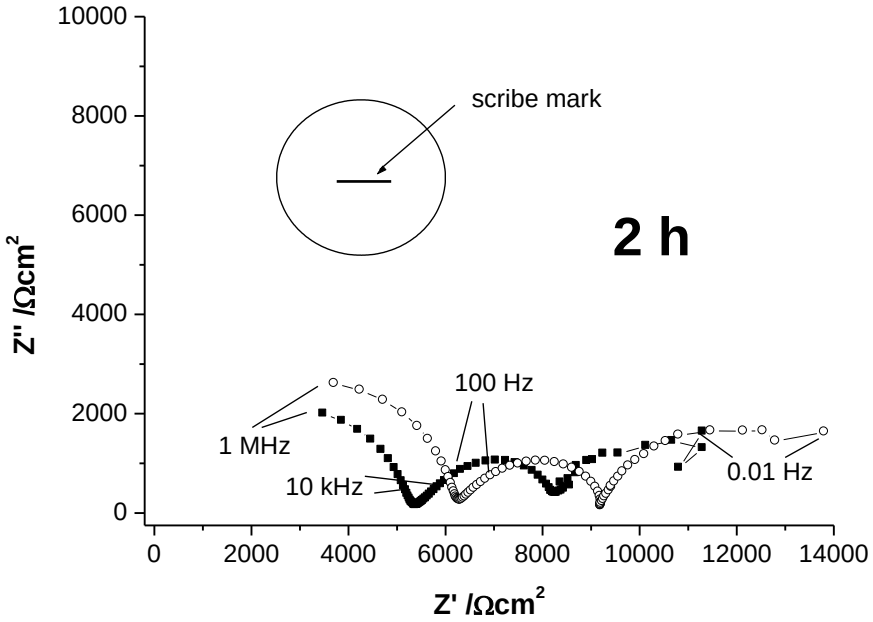

Fig. 13. Impedance spectra in Nyquist format for coatings cured in a magnetic field (●) and without a magnetic field (o) with artificial damage after 2h of immersion in dilute Harrison's solution.

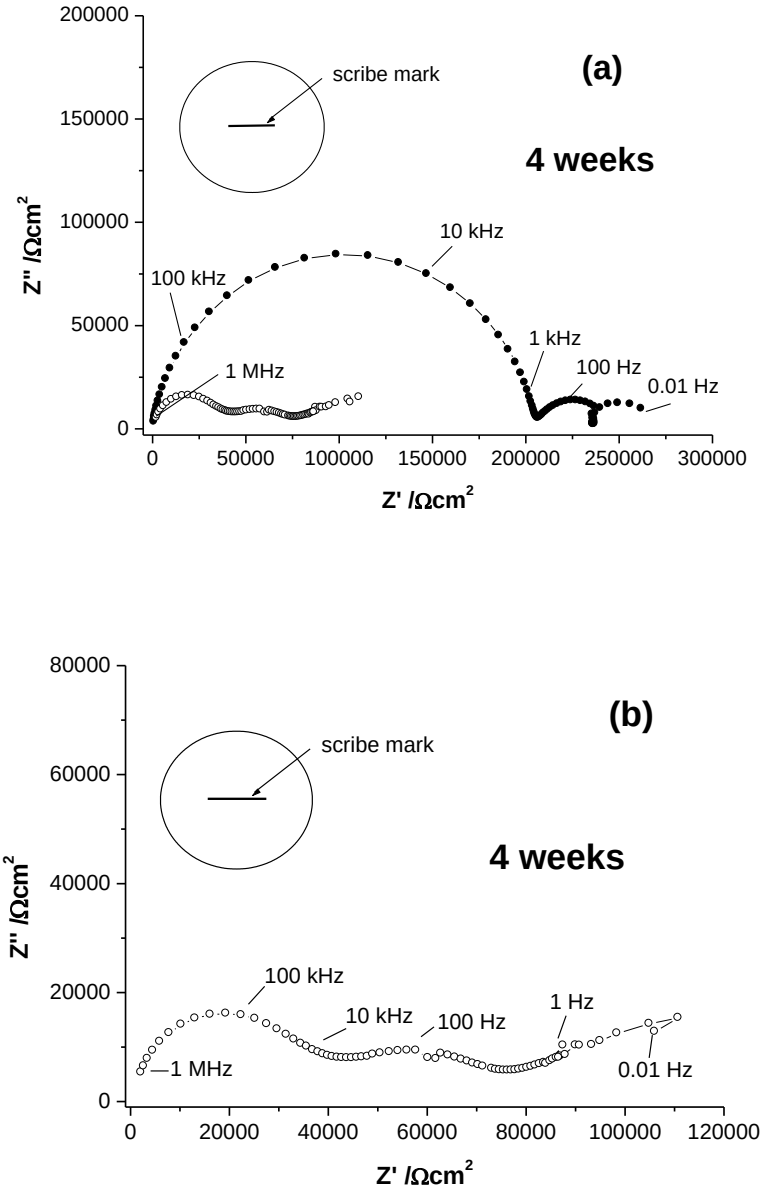

Fig. 14. Impedance spectra in Nyquist format for coatings cured in a magnetic field (●) and without a magnetic field (o) with artificial damage after 4 weeks of immersion in dilute Harrison's solution (a) and enlarged spectrum from (a) for the coating cured without the presence of the magnetic field.

5. Summary

A new method of obtaining stratification of properties within one coating layer has been proposed. For this purpose, a magnetic field and magnetic pigment in the form of nickel ferrite was used. In general, ferrites have the characteristics of active anti-corrosive pigment, some of them have magnetic properties, necessary for this application. The aim of the magnetically targeted anti-corrosive pigment delivery system is to carry the pigment particles to the place of their action, in the case of active anti-corrosive pigments near the interface metal substrate/coating.

The following conclusions can be drawn from the performed tests:

- The stratification of magnetic ferrite pigment particles in the epoxy coating in the magnetic field was confirmed.
- An epoxy coating containing nickel ferrite as a magnetic pigment subjected to a magnetic field during curing of the coating causes changes in its electrical and dielectric properties.
- A dispersion of the electric capacity of the coating exposed to the magnetic field during curing is observed.
- The ferrite pigment in the epoxy coating exposed to the magnetic field during curing of the coating has a more favourable anti-corrosive effect compared to an identical coating hardened traditionally, without the presence of a magnetic field.

Magnetic particles possess a great promise in the improvement of protective coating systems due to their unique properties and can be used to overcome some problems and prevent the limitations of present solutions in this area.

References

[1]. U. Poth, Automotive Coatings Formulation: Chemistry, Physics und Practices, Vincentz Network, 2008.

[2]. Handbook of Smart Coatings for Materials Protection, A.S.H. Makhlouf (ed.), Elsevier, Woodhead Publishing, 2014.

[3]. M.S. Okyere, Corrosion protection for the oil and gas industry: pipelines, subsea equipment, and structures, CRC Press, 2019.

[4]. W. Funke, How Organic Coating Systems Protect Against Corrosion, Polymeric Materials for Corrosion Control; Dickie, R. (ed.); ACS Symposium Series; American Chemical Society: Washington, DC, 1986, 222-228.

[5]. Ch. Carr, E. Wallstom, Theoretical aspects of self-stratification, Prog. Org. Coat. 28 (1996) 161-171.

[6]. E. Langer, H. Kuczynska, E. Kaminska-Tarnawska, J. Łukaszczyk, Self-stratifying coatings containing barrier and active anticorrosive pigments, Prog. Org. Coat. 71 (2011) 162–166.

[7]. A. Beaugendre, S. Degoutin, S. Bellayer, C. Pierlot, S. Duquesne, M. Casetta, M. Jimenez, Self-stratifying coatings: A review, Prog. Org. Coat. 110 (2017) 210–241.

[8]. S. Zahedi, D. Zaarei, S. R. Ghaffarian, Self-stratifying coatings: a review, J. Coat. Technol. Res., 15 (2018) 1–12.

[9]. S. Zahedi, D. Zaarei, S.R. Ghaffarian, M. Jimenez, A new approach to design self stratifying coatings containing nano and micro pigments, J. Disper. Sci. Technol. (2019), DOI: 10.1080/01932691.2019.1614032.

[10]. A. Kalendová, J. Brodinová, Spinel and rutile pigments containing Mg, Ca, Zn and other cations for anticorrosive coatings, Anti-Corros. Method. M. 50 (2003) 352-363.

[11]. M. Zubielewicz, W. Gnot, Mechanisms of non-toxic anticorrosive pigments in organic waterborne coatings, Prog. Org. Coat. 49 (2004) 162–166.

[12]. A. Miszczyk and K. Darowicki, Study of anticorrosion and microwave absorption properties of NiZn ferrite pigments, Anti-Corros. Method. M. 58 (2011) 13–21.

[13]. A. Miszczyk, Protective and suppressing electromagnetic interference properties of epoxy coatings containing nano-sized NiZn ferrites, Front. Mater. 7 (2020) 183.

[13]. A.H. Morrish, The Physical Principles of Magnetism, IEEE Press, 1980.

[14]. D. Jiles, Introduction to Magnetism and Magnetic Materials, Springer-Science+Business Media, 1991.

[15]. C-G. Stefanita, Magnetism. Basics and Applications, Springer, 2012.

[16]. Z. Xu, H. Wu, Q. Wang, S. Jang, L. Yi, J. Wang, Study on movement mechanism of magnetic particles in silicone rubber based magnetorheological elastomers with viscosity change, J. Magn. Magn. Mater. 494 (2020) 165793.

[17]. T.E. Faber, Fluid Dynamics for Physicists, Cambridge University Press, 1995.

[18]. L.A. Kafshgari, M. Ghorbani, A. Azizi, Synthesis and characterization of manganese ferrite nanostructure by co-precipitation, sol-gel, and hydrothermal methods, Particul. Sci. Technol. 37 (2019) 900-906.

[19]. J.B Harrison, T.C.K. Tickle, New aspects of the atmospheric corrosion of steel and their implications, Journal of Oil Colour Chemists Association, 45 (1962) 571-580.

[20]. F.D. Timmins, Avoiding paint failures by prohesion. Journal of Oil Colour Chemists Association, 62 (1979) 131-139.

[21]. N.D. Cremer, The move to cyclic salt-spray testing from continuous salt spray, Anti-Corros. Method. M. 43(3) (1996) 16-20.

[22]. S.B. Lyon, G.E. Thompson, J.B. Johnson, Materials evaluation using wet-dry mixed salt-spray tests, New methods for corrosion testing of aluminum alloys, ASTM STP 1134, ASTM, Philadelphia, 1992, 20-31.

[23]. M. Zapponi, T. Perez, C. Ramos, C. Saragovi, Prohesion and outdoors tests on corrosion products developed over painted galvanized steel sheets with and without Cr(VI) species, Corros. Sci. 47 (2005) 923–936.

[24]. R.L. Howard, S.B. Lyon, J.D. Scantlebury, Accelerated tests for the prediction of cut-edge corrosion of coil-coated architectural cladding. Part I: cyclic cabinet salt spray, Progress in Organic Coatings 37 (1999) 91-98.

[25]. G. Bierwagen, D. Tallman, J. Li, L. Hea, C. Jeffcoate, EIS studies of coated metals in accelerated exposure, Prog. Org. Coat. 46 (2003) 148–157.

[26]. O.O. Knudsen, A. Forsgren, Corrosion control through organic coatings, Second edition, CRC Press, Taylor & Francis Group, Boca Raton, London, New York, 2017, chapter 15.

[27]. J. Lin, D. Battocchi, G.P. Bierwagen, Degradation of magnesium-rich primers over AA2024-T3 during constant immersion in different solutions, Corrosion 73 (2017) 408-416.

[28]. T. Sasmaz Kuru, M. Kuru, S. Bagci, Structural, dielectric and humidity properties of Al-Ni-Zn ferrite prepared by co-precipitation method, J. Alloy. Comp. 753 (2018) 483-490.

[29]. C. Suryanarayana, M. G. Norton, X-Ray Diffraction: A Practical Approach, Springer-Science+Business Media, 1998.

[30]. SME Mineral Processing & Extractive Metallurgy Handbook, R.C. Dunne (ed.), Society for Mining, Metallurgy & Exploration, Englewood Colorado, USA, 2019, 9.

[31]. V.F. Lvovich, Impedance Spectroscopy. Applications to Electrochemical and Dielectric Phenomena, Wiley, 2012.

Data Availability

The raw/processed data required to reproduce these findings cannot be shared at this time as the data also forms part of an ongoing study.